AIP | Applied Physics Letters

Recovery improvement of graphene-based gas sensors functionalized with nanoscale heterojunctions

Il-Suk Kang, Hye-Mi So, Gyeong-Sook Bang, Jun-Hyuk Kwak, Jeong-O Lee et al.

Citation: Appl. Phys. Lett. **101**, 123504 (2012); doi: 10.1063/1.4753974
View online: http://dx.doi.org/10.1063/1.4753974
View Table of Contents: http://apl.aip.org/resource/1/APPLAB/v101/i12
Published by the American Institute of Physics.

Recovery improvement of graphene-based gas sensors functionalized with nanoscale heterojunctions

Il-Suk Kang,[1] Hye-Mi So,[1] Gyeong-Sook Bang,[1] Jun-Hyuk Kwak,[1] Jeong-O Lee,[2] and Chi Won Ahn[1,a)]
[1]*National Nanofab Center, Korea Advanced Institute of Science and Technology, Daejeon 305-806, Korea*
[2]*Korea Research Institute of Chemistry Technology, Daejeon 305-600, Korea*

(Received 17 July 2012; accepted 5 September 2012; published online 18 September 2012)

We report a development of reduced graphene oxide (rGO)-based gas sensors with a practical recovery by facile functionalization with tin dioxide nanoclusters. Upon the introduction of UV illumination to this nanostructure, the reaction on surfaces of tin dioxide nanoclusters was activated and thereby the nanoscale heterojunction barriers between the rGO sheet and the nanoclusters were developed. This lowered the conductance to quickly recover, which was intensified as the cluster density has reached to the percolation threshold. However, after the formation of the cluster percolating network, the sensor response has totally changed into a deterioration of the sensitivity as well as the recovery. © *2012 American Institute of Physics*. [http://dx.doi.org/10.1063/1.4753974]

Functionalization of graphene sheets with nanoclusters (NCs) can potentially display additional properties due to the interaction between the NCs and the graphene.[1]

Electron transport through graphene is highly sensitive to adsorbed molecules owing to the two-dimensional structure of graphene that makes every carbon atom a surface atom. Graphene has been demonstrated as a promising gas-sensing material. The gas-sensing mechanism of graphene is generally ascribed to the adsorption/desorption of gaseous molecules (which act as electron donors or acceptors) on the graphene surface.[2] Particularly, in reduced graphene oxide (rGO), the gas molecule adsorbs on the rGO surface with the oxygen functional groups through hydrogen bonding, and then electron transfers to the rGO resulting in a change of the resistance.[3] To generate a decent sensing signal, a suitable amount of functional groups are needed to act as the adsorption site, which makes the rGO quite distinguished from a zero-gap graphene.[4] Since too many functional groups would significantly reduce the conductivity of the rGO, Zhang *et al.* showed that such balance was realized on a 300 °C-annealed rGO.[5]

However, the desorption rate is found to be slower than the adsorption rate, which can be attributed to the reaction occurred on the graphene surface.[6] Particularly, in rGO, remnant high-energy adsorption sites, e.g., the oxygen functional groups should result in higher binding energies, which makes the desorption slower.[3] The heating significantly accelerates the desorption process, by exciting the molecules vibrationally so that they enter a repulsive state.[7] And UV illumination expedites the desorption of molecules.[6] Therefore, the integration with a micro-joule heater or a UV-light emitting diode can be elegant approaches without the device bulky and complicated.

Recently, gas-sensing properties of graphene sheets functionalized with NCs have been reported. Mao *et al.* showed an rGO gas sensor with tin oxide (SnO_2) NCs.[8] However, only functionalization with SnO_2 NCs did not solve the recovery problem. SnO_2 is well known to be an n-type gas-sensing material activated by heat or UV.[9] Accordingly, for a practical recovery, we designed an rGO sheet with a facile, noncovalent immobilization of SnO_2 NCs under UV illumination at room temperature. We found this functionalized rGO sheet readily allowing more than an order of magnitude improvement in the recovery over the pristine rGO sheet.

Graphene oxide were prepared using a procedure previously reported.[5] Thermal reduction of the graphene oxide was carried out in a tube furnace at 300 °C in hydrogen atmosphere for 1 h. Figure 1(a) shows a scanning electron microscope (SEM) image of a typical device with a few-layered rGO sheet bridging a pair of electrodes. X-ray photoelectron spectroscopy (XPS) measurement (Fig. 1(b)) shows that the rGO sheet had some amount of oxygen functional groups. Then, Sn NCs were immobilized on the rGO device in order to create nanoscale heterojunctions. The immobilization process was based on an inert-gas condensation that our group previously reported.[10] The operating parameters were optimized to produce Sn NCs of 12.0 ± 0.5 nm in diameter, as shown in Fig. 1(c).

The density of the clusters was controlled by the functionalization time. The evolution of conductance with increasing the functionalization time of Sn NCs on the rGO device was real-time monitored, as shown in Fig. 1(d). The observed evolution is similar to other cluster deposition experiments.[10,11] The inset shows that the fluctuation in the differential conductance begins to increase between 55 and 60 min, which is attributed to the formation of the percolating network of Sn NCs. We call this onset time "percolation threshold," and after that, the conductance has dramatically increased by about 2.5 orders of magnitude. Accordingly, we used four functionalization conditions of 5, 30, 55, and 60 min.

There are two main oxides of Sn: stannic oxide (SnO_2) and stannous oxide (SnO).[12] The oxidation of small clusters is thought to proceed slowly with the formation of first SnO and then SnO_2.[13] To speed up this process, we annealed the

a)E-mail: cwahn@nnfc.re.kr.

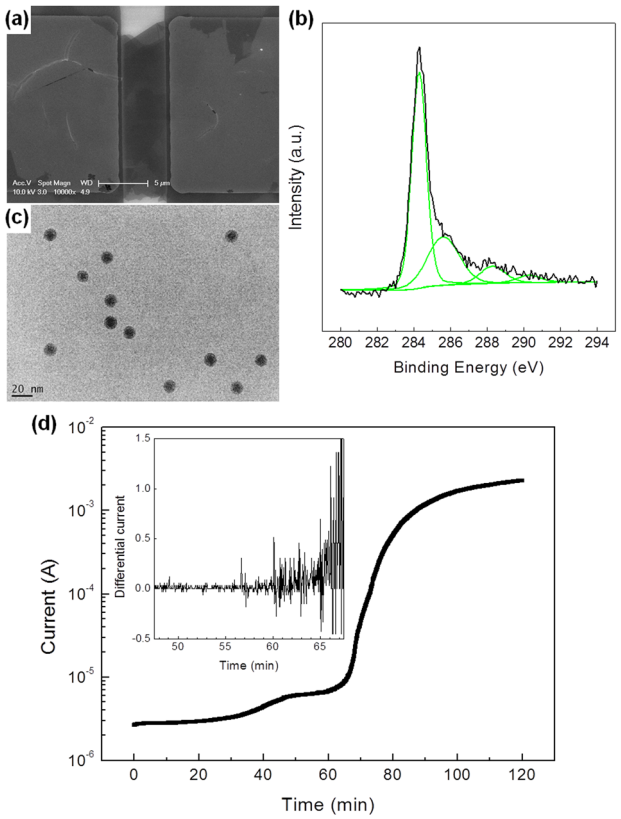

FIG. 1. (a) SEM image showing a few-layered rGO sheet bridging a pair of gold electrodes. (b) C1s XPS spectra of the rGO sheet. The binding energies are 284.3, 285.7, 288.2, and 290.2 eV for C-C, C-O, C═O, and C(O)O, respectively. (c) TEM image of Sn NCs on a TEM grid with 1 min deposition. (d) Real-time conductance measurement during the functionalization of the rGO sheet with Sn NCs in a vacuum at room temperature. Inset: the differential conductance.

Sn NCs at 200 °C in ambient air. For determining the annealing time, the real-time conductance measurement of a percolated Sn NC film without an rGO sheet was carried out during the annealing, as shown in Fig. 2. Upon annealing at 200 °C, a dramatic decrease in conductance was observed at around 10 min, and the conductance was recovered almost to the original value at ~20 min. Several different factors may be responsible for this result: the NCs may sinter and form

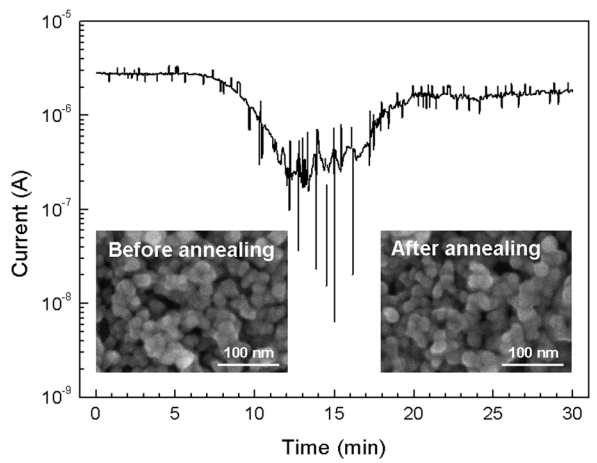

FIG. 2. Real-time conductance measurement of a percolated Sn NC film without an rGO sheet during the annealing at 200 °C in ambient air. Inset: SEM images of the film before and after the annealing, respectively.

larger agglomerates, and/or the oxidation state of the NCs may be altered (SnO_2 is electrically much more conductive than SnO).[11] SEM images (the inset of Fig. 2) show that the NC diameters are not significantly altered by the annealing process. This supports that the annealing procedure is responsible for changing the oxidation state of the individual NCs rather than changing the morphology of the film (sintering). Therefore, this conductance result indicates that the Sn NCs were transformed via SnO into SnO_2 within 20 min. Accordingly, we set the annealing time of 30 min as an optimized condition.

The device was periodically exposed to 100 ppm NO_2 in nitrogen for 500 s to register a sensing signal, followed by 1300 s of purge with nitrogen to recover the device. First, a graphene oxide sheet before the reduction showed no response to NO_2 (not shown). After being reduced, the graphene oxide sheet became much more responsive to NO_2, as shown in Fig. 3(a). Upon the introduction of NO_2, the pristine rGO device showed an increase in conductance (sensitivity = 3.84%). The sensitivity and the recovery are evaluated as the ratio of $(G_g - G_b)/G_b$ and that of $-(G_a - G_g)/(G_g - G_b)$, respectively, where G_g is the sensor conductance in NO_2, and G_b and G_a are conductances in N_2 purging before and after the NO_2 exposure, respectively. "Recovery = 100%" means the conductance is recovered to the initial value ($G_a = G_b$). Figures 3(c) and 3(d) show the comparison of the sensitivity and the recovery of devices, respectively. NO_2 is a strong oxidizer with the electron-withdrawing power[14] and it is well known that rGO sheets prepared by the thermal reduction show the p-type behavior;[15] therefore, the electron transfer from the rGO sheet to the adsorbed NO_2 molecule leads to an enriched hole concentration and enhanced electrical conduction of the rGO sheet. However, even with an ample amount of N_2 purging, the conductance of the pristine rGO device was only partially recovered (recovery = 7.29%). Accordingly, the sensitivity in the next cycle has decreased by as much as 74%. Figure 3(a) shows UV illumination accelerates the recovery, as mentioned above. Although the base value of the conductance and the sensitivity were lower, the recovery of the pristine rGO sheet under UV illumination was more than 5 times higher than without UV illumination. Before the functionalization with NCs, it is required to investigate the effects of the annealing for fabricating SnO_2 NCs on the sensor response of the rGO sheet. In Fig. 3(a), further annealing (150 min) did not change the signal (by less than 10% improvement in recovery). Considering that the recovery was improved by more than 60% after adding low-density (just 5 min) SnO_2 NCs on the annealed rGO sheet, the effect of the annealing can be ignored when analyzing the recovery.

The functionalization with SnO_2 NCs did not improve the sensitivity, let alone the recovery, contrary to the results of Ref. 8 (not shown). It is likely that the heterojunction barrier between the rGO sheet and the NCs fabricated in this study is lower than in Ref. 8. Figure 3(b) shows the sensor response under UV illumination as a function of the functionalization time (SnO_2 NC density). As the functionalization time has increased, the recovery has dramatically increased. Particularly, in the device with the NC density vicinal to the percolation threshold (55 min), the full recovery was achieved under the same purge condition. However, after the

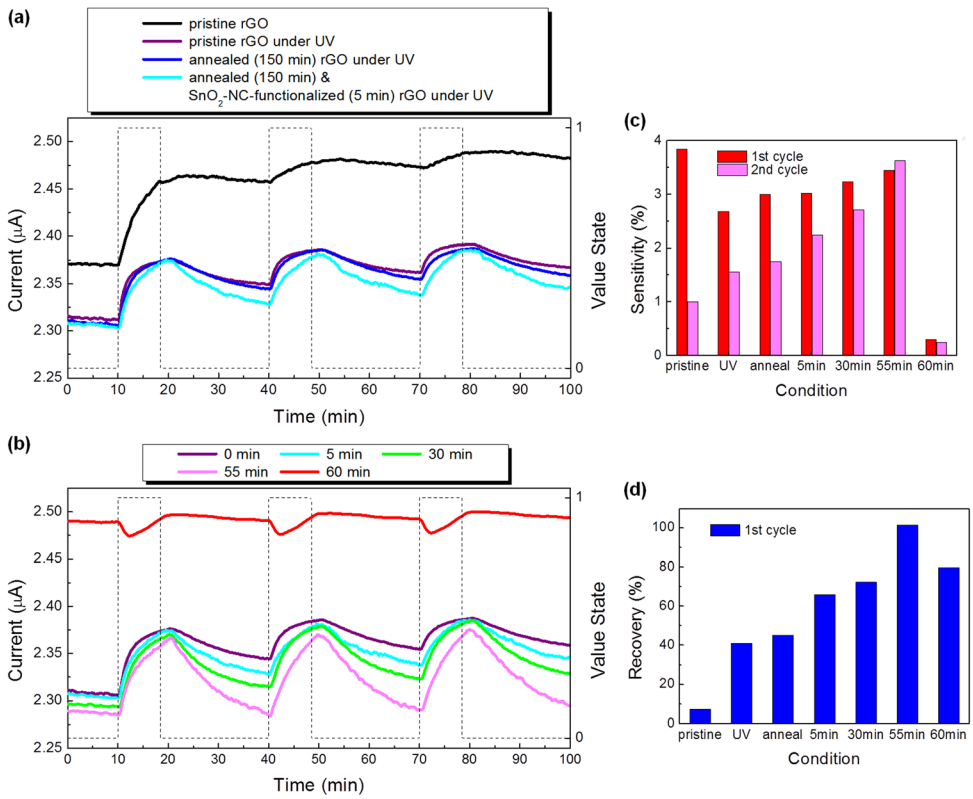

FIG. 3. Sensor responses from various rGO devices. (a) The effect of annealing, UV illumination, and functionalization on a pristine rGO. (b) The effect of functionalization time (SnO_2 NC density) under UV illumination. The NO_2 concentration is 100 ppm in nitrogen. Comparison of (c) the sensitivity and (d) the recovery of every condition in (a) and (b).

percolation threshold (60 min), the sensor response has totally changed. The overall increase of conductance has observed, and the sensitivity has decreased by 91% as well as the recovery by 22%, compared to those of the 55 min-functionalized device. It is also noted that upon the introduction of NO_2, the decrease of conductance was observed, which is the n-type behavior not being found in devices with NC densities below the percolation threshold.

Figure 4 shows schematic diagrams of the change in the electrical conduction of the devices simplified with one-dimensional SnO_2 NC array on the rGO sheet, when NO_2 is off. As mentioned above, the conduction of the pristine or unfunctionalized rGO device can be recovered only through

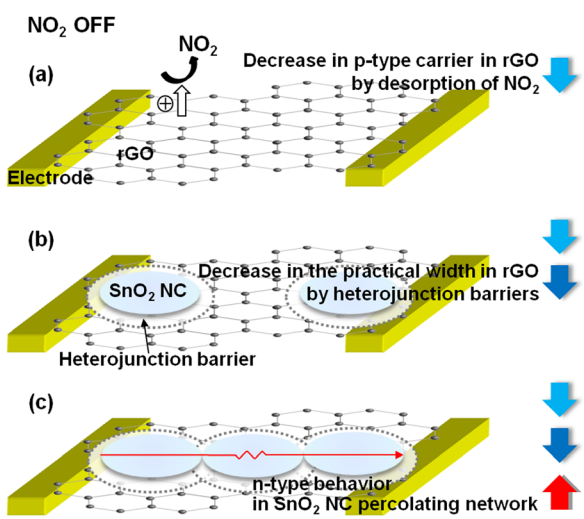

FIG. 4. Schematic diagrams of the change in the electrical conduction of rGO devices, when NO_2 is off; (a) no SnO_2 NCs, (b) isolated SnO_2 NCs, and (c) SnO_2 NC percolating network. Arrows indicate the increase or the decrease in conductance.

the decrease in the hole concentration by the desorption of NO_2, as shown in Fig. 4(a). When NO_2 is off, i.e., when the electron is doped into the UV-activated SnO_2 NC from NO_2, this lowers the work function of the NCs and thereby heterojunction barriers are developed. In other words, the hole depletion zone widens, which reduces the practical width of the conduction channel in the rGO sheet, as shown in Fig. 4(b). Finally, this effect accelerates the decrease in conductance, which is intensified as the cluster density reaches to the percolation threshold. In the percolated devices such as the 60 min-functionalized device, the n-type response behavior of the SnO_2 NC percolating network becoming another electrical pathway between the electrodes is reflected in the sensor response, as shown in Fig. 4(c). Accordingly, the sensitivity and the recovery have deteriorated, and upon introduction of NO_2, the decrease of conductance was observed in Fig. 3(b).

In summary, we designed an rGO gas sensor functionalized with SnO_2 NCs in order to improve the recovery performance. Through the measurement of the sensor response to dilute NO_2 as a function of the NC density under UV illumination, we found that the rGO device functionalized near the percolation threshold showed the best recovery, and then the best sensitivity at succeeding cycles. This can be rationalized by the modulation of the nanoscale heterojunction barriers by activating the reaction on SnO_2 NC surfaces with UV illumination. This finding is encouraging for further higher performance gas sensors on the base of more optimized nanostructures by the versatile synthesis approaches.

This work was supported by a grant from the Development of Infrastructure for Nano-Graphene Devices Program (Code No. 2011-0017333) and the Center for Advanced Soft Electronics under the Global Frontier Research Program

(Code No. 2011-0032147) of the Ministry of Education, Science and Technology, Korea.

[1]P. V. Kamat, J. Phys. Chem. Lett. **1**, 520 (2010).
[2]F. Schedin, A. K. Geim, S. V. Morozov, E. W. Hill, P. Blake, M. I. Katsnelson, and K. S. Novoselov, Nature Mater. **6**, 652 (2007).
[3]J. T. Robinson, F. K. Perkins, E. S. Snow, Z. Wei, and P. E. Sheehan, Nano Lett. **8**, 3137 (2008).
[4]H. Chang, Z. Sun, Q. Yuan, F. Ding, X. Tao, F. Yan, and Z. Zheng, Adv. Mater. **22**, 4872 (2010).
[5]L. S. Zhang, W. D. Wang, X. Q. Liang, W. S. Chu, W. G. Song, W. Wang, and Z. Y. Wu, Nanoscale **3**, 2458 (2011).
[6]G. Ko, H.-Y. Kim, J. Ahn, Y.-M. Park, K.-Y. Lee, and J. Kim, Curr. Appl. Phys. **10**, 1002 (2010).
[7]F. Yang, D. K. Taggart, and R. M. Penner, Small **6**, 1422 (2010).
[8]S. Mao, S. Cui, G. Lu, K. Yu, Z. Wen, and J. Chen, J. Mater. Chem. **22**, 11009 (2012).
[9]D. Haridas, A. Chowdhuri, K. Sreenivas, and V. Gupta, Sens. Actuators B **153**, 152 (2011).
[10]I.-S. Kang, H.-S. Seo, D.-H. Kim, T.-Y. Lee, J.-M. Yang, W.-J. Hwang, and C. W. Ahn, J. Nanosci. Nanotechnol. **10**, 3667 (2010).
[11]A. Lassesson, M. Schulze, J. van Lith, and S. A. Brown, Nanotechnology **19**, 015502 (2008).
[12]M. Batzill and U. Diebold, Prog. Surf. Sci. **79**, 47 (2005).
[13]C. H. Shek, J. K. L. Lai, G. M. Lin, Y. F. Zheng, and W. H. Liu, J. Phys. Chem. Solids **58**, 13 (1997).
[14]J. A. Robinson, E. S. Snow, S. C. Badescu, T. L. Reinecke, and F. K. Perkins, Nano Lett. **6**, 1747 (2006).
[15]I. Jung, D. A. Dikin, R. D. Piner, and R. S. Ruoff, Nano Lett. **8**, 4283 (2008).